POLITECNICO DI TORINO
Repository ISTITUZIONALE

Development and 3D Printing of AESO-Based Composites Containing Olive Pit Powder

Terms of use:

Publisher copyright

(Article begins on next page)

29 September 2025

Article

Development and 3D Printing of AESO-Based Composites Containing Olive Pit Powder

Giovanna Colucci [1,2,*], Francesca Sacchi [1,2], Marta Checchi [3], Marianna Barbalinardo [4], Francesca Chiarini [3], Federica Bondioli [1,2], Carla Palumbo [3] and Massimo Messori [1,2]

[1] Department of Applied Science and Technology (DISAT), Politecnico di Torino, Corso Duca Degli Abruzzi 24, 10129 Torino, Italy; francesca.sacchi@polito.it (F.S.); federica.bondioli@polito.it (F.B.); massimo.messori@polito.it (M.M.)

[2] National Interuniversity Consortium of Materials Science and Technology (INSTM), Via G. Giusti 9, 50121 Firenze, Italy

[3] Department of Biomedical, Metabolic and Neural Sciences, Section of Human Morphology, Università di Modena e Reggio Emilia, Largo del Pozzo 71, 41124 Modena, Italy; marta.checchi@unimore.it (M.C.); francesca.chiarini@unimore.it (F.C.); carla.palumbo@unimore.it (C.P.)

[4] Consiglio Nazionale Delle Ricerche, Istituto per lo Studio dei Materiali Nanostrutturati (CNR-ISMN), via P. Gobetti 101, 40129 Bologna, Italy; marianna.barbalinardo@cnr.it

[*] Correspondence: giovanna.colucci@polito.it

Abstract

Bio-based polymeric composites were prepared by dispersing different amounts of olive pit (OP) powder within an acrylate epoxidized soybean oil (AESO) photocurable resin using tetrahydrofurfuryl acrylate (THFA) as diluent and (2,4,6-trimethylbenzoyl), phosphine oxide (BAPO) as photo-initiator, and they were photocured by Vat Photopolymerization (VP) using a Liquid Crystal Display (LCD) 3D printer. Formulation viscosity was studied because of its important role in a VP process able to influence the printability of the final parts. Different 3D printed architectures were successfully realized with good resolution and accuracy, high level of detail, and flexibility. The effect of OP addition was investigated by thermal (TGA and DSC), morphological (SEM and PSD), viscoelastic (DMA), and mechanical (tensile testing) characterization. The filler led to an increase in the T_g, storage modulus, and tensile properties, underlining the stiffening effect induced by the OP particles onto the polymeric starting resin. This underlines the possibility to apply these bio-based composites in many application fields by valorizing agro-wastes, developing more sustainable materials, and taking advantages of VP 3D printing, such as low costs, minimal wastage, and customized geometry. Biocompatibility tests were also successfully carried out. The results clearly indicate that the AESO-based composites promote cell adhesion and viability.

Keywords: olive pit; acrylate epoxidized soybean oil (AESO); 3D printing; vat photopolymerization (VP); liquid crystal display (LCD)

1. Introduction

The agro-industrial economy of many South Mediterranean countries is mostly based on olive oil production and olive processing [1]. Virgin olive oil is extracted from olives using exclusively mechanical techniques, which include the crush of the fruit to allow oil release, the malaxation of the olive paste to induce oil drop coalescence, and the mechanical recovery of the oil by pressing [1–3]. During the whole supply chain of olive oil processing, a variety of products are generated, such as olive pomace, olive leaves, and olive stones

and seeds. A major problem which significantly affects the environmental sustainability of the extraction process is the disposal of residues and waste [4,5]. Their quality and quantity are closely correlated to the waste and by-products produced. The olive stone, also known as olive pit (OP), is a solid residue to dispose of, and it represents about 18–25% of the total olive weight [4]. It is a lignocellulosic material characterized by a complex structure made of microfibrils, whose main components are hemicellulose, cellulose, and lignin. It represents the internal part of the drupe, which is crushed and eliminated with waste during olive milling [2].

The OP can be considered the result of the elimination of the olive whole stone from the olive paste, an operation carried out to obtain sweeter olive oil, more stable to the oxidation. Moreover, it can be obtained from the dedusting of the exhausted olive husk coming from olive husk factories [2]. The size and shape of the OP particles strictly depend on the milling process adopted, while the quantity ranges from 25 to 40% of the weight of the pressed olives, according to the used extraction technology [2,3]. In this context, considering that the price of raw materials has continuously increased during the last years, due to unsustainable linear economy, this kind of resource is becoming more precious [2–5]. The environment is being irreparably scarred, and waste are greatly increasing. As a counteroffensive to these phenomena, a new type of economy, defined as "circular", is developing. Bio-based materials, coming from sustainable and renewable sources, are developed and applied to replace petroleum-based products, with the purpose to optimize waste management systems [6]. The application of natural fillers or fillers deriving from industrial trash and agro-waste is attracting great interest in the field of composite materials [7,8]. Nowadays, agricultural waste represents an important resource for the development of fillers, which can add value to the polymeric composite products, reducing their production costs.

The available literature reports an estimation of the percentage of bio-based feedstocks used in the manufacturing of polymeric products rising from 5% in 2004 to 12% in 2010, and then to about 18% in 2020. The study predicts further 25% growth in use in 2030 [9]. Considering these aspects, the industrial sector is increasingly turning to the application of bio-based fillers in polymeric materials. At the same time, the high amount of waste generated by the agro-industrial field can be applied as a cost-effective and valuable filler. Almond shell, pistachio nutshell, apricot, peanut shell, avocado seed, and coconut shell represent examples of powders studied and employed as biofillers for the improvement of the final properties of polymer matrix composites [10,11].

It has been estimated that OP production in Europe is around 6,8 million tons per year [12]. For this reason, it can be widely employed as a reinforcing filler in many industrial applications, like coatings, additives, constructions, and cosmetics [9–15]. The literature describes an interesting re-use of the OP as an additive in cement mortar to improve its thermal insulation efficiency. Many studies also report the use of OP powder to produce activated carbon and sugar [9,13], metal bio-adsorbents [14], and in the automotive field, it is used as an abrasive or again for recovering the agro-waste to produce biofuel from renewable sources [6,15]. Moreover, olive stone derivatives can be employed as fillers in polymers, such as thermoplastics and thermosets, with the aim of reducing the environmental impact of bio-based components [15,16].

The introduction of OP powder into a polymer can result in a rise of the elastic modulus of the composite material, with the outcome of reduced tensile strength and elongation at break. However, despite OP characteristics, this bio-based material has never been considered as a filler in polymer composites for applications in 3D printing (3DP). A long list of papers is present in the literature on the preparation and characterization of polymeric composites obtained by 3DP by adding biofillers or agro-waste [17–19]. In

fact, 3DP includes a set of highly versatile and low-cost tools able to prototype and realize three-dimensional components with high design versatility, structural complexity, and dimensional accuracy. A polymeric part can be built layer by layer until the desired object is reproduced in a very short time by using lower amounts of raw materials and reducing final costs [20–24].

The authors themselves in previous studies have investigated the effect of the addition of agro-waste coming from corn and wine byproducts and lignin on the final properties of acrylate epoxidized soybean oil (AESO) resin, successfully realizing 3D printed parts by using a Liquid Crystal Display (LCD) 3D printer [18,19]. The obtained results underline the possibility to develop polymeric materials showing highly crosslinked structures with tunable properties, varying from rigid to flexible, useful for many applications, above all automotive or biomedical.

The present paper aims to weigh the possibility of using for the first-time OP powder to develop bio-based composites by 3DP using the LCD as VP technology. The novelty introduced with this paper is preparation, characterization, and successful printing via LCD of novel polymeric composites, where different amounts of OP powder are added within soybean oil-based resin. The use of LCD matches the sustainability of AM technologies with that related to the bio-based materials employed.

2. Materials and Methods

2.1. Materials

Liquid photocurable formulations were prepared mixing acrylate epoxidized soybean oil (AESO) as bio-based thermoset resin, tetrahydrofurfuryl acrylate (THFA) as reactive diluent, and phenyl bis (2,4,6-trimethylbenzoyl) phosphine oxide (BAPO) as radical photo-initiator, all purchased by Merck (Darmstadt, Germany).

The AESO resin is a commercial monomer which offers several advantages as a renewable and multifunctional resin for photocuring applications, making it a promising alternative to conventional petroleum-based monomers. One of the most significant advantages is its bio-based origin. AESO is derived from soybean oil and contributes to the development of more sustainable materials, aligning with the increasing demand for greener monomers and reduced carbon footprints in polymer manufacturing [25–27]. AESO molecules possess multiple acrylate functionalities, which allow for efficient crosslinking under UV irradiation, useful for VP printing processes. This enables the formation of crosslinked polymer networks without the need for elevated temperatures or long curing times. Additionally, the presence of long aliphatic chains from the soybean oil backbone imparts flexibility and strength to the final photocured polymer. Furthermore, AESO's low toxicity compared with other acrylates makes it a safer alternative option for many specific application requirements [28–30].

Due to its high viscosity not compatible for the VP printing process, THFA was added to the resin. THFA is an environmentally friendly acrylic monomer that contains a tetrahydrofuran ring in its chemical structure. It is obtained from biomass by the hydrogenation of hemicellulose. THFA was added to the liquid resin as reactive diluent to decrease the AESO viscosity into the optimal range for the 3D printing process via LCD VP. Moreover, it also actively participates in the polymerization reaction, becoming an integral part of the final crosslinked polymer network [18,19].

OP powder, an agro-waste by-product coming from olive oil industry, supplied by RIMSA Metal Technology SL (Barcelona, Spain), was used as a biofiller.

2.2. Photocurable Formulations

AESO-based formulations were obtained by combining the liquid resin with THFA (60:40 mass ratio) in the presence of 2 wt.% of BAPO. This ratio was selected after several rheological tests performed by varying the AESO and THFA content from 100 to 0 wt.%, as it resulted in a viscosity close to the optimal value required for the VP process [18,19,27], thus ensuring good printability via LCD. The bio-based composites were obtained by dispersing OP powder at 5 and 7.5 wt.% to the AESO-THFA formulation. The OP powder was previously dried in an oven at 80 °C for 8 h and then added to the resin by alternating between 30 min of magnetic stirring and 30 min of ultrasonic bath for a total of 3 h. The obtained samples are coded as AESO-THFA+O5 and AESO-THFA+O7.5, respectively.

2.3. Three-Dimensional Printing of Unfilled and Filled Samples

The AESO-based formulations were 3D printed by using a Phrozen Sonic Mini 8K (Phrozen, Hsinchu City, Taiwan) vat polymerization LCD 3D printer. Exposure time, layer thickness, and speed were set using Chitubox Software. v1.9.5. The printing parameters were optimized for each formulation to study their printability. The 3D printed samples were removed from the build platform, washed with 1-butanol, and post-cured for 30 min using an Anycubic Wash&Cure Plus machine (Anycubic Technology Co., Hongkong).

2.4. Characterization

The particle size distribution of OP powder was evaluated by using an automated particle size and shape analyzer Morphology 4 (Malvern Panalytical Ltd., Malvern Worcestershire, UK). The tests were carried out on a volume of 3 mm^3 of dry powder dispersed onto a glass plate, with injection time of 10 ms and a high-pressure dispersion of 4 bar.

The unfilled and filled sample microstructures were studied using a Phenom™ XL Scanning Electron Microscope (Thermo Fisher Scientific, Waltham, MA, USA) at a voltage of 15 kV after metallization with platinum.

Thermal properties of the OP powder and the photocured samples were evaluated by thermogravimetric analysis (TG) using a Mettler-Toledo TGA 851e Instrument (Columbus, OH, USA), from 25 to 800 °C with a heating rate of 10 °C min^{-1} under an air flux (50 mL min^{-1}), and by differential scanning calorimetry (DSC) analysis by using a Netzsch 214 Polyma Equipment (Selb, Germany) from −50 to 250 °C with a heating/cooling rate of 10 °C min^{-1} under a nitrogen flow of 40 mL min^{-1}. Two heating scans and one cooling scan were recorded.

The viscosity of the AESO-based formulations was evaluated at 25 °C by using an Anton Paar MCR 702e MultiDrive Rheometer (Graz, Austria) in a parallel plate configuration.

The gel content of the photocured samples was calculated according to the ASTM D2765-84 standard, after 24 h of extraction in chloroform [31].

Dynamic-mechanical analysis (DMA) was carried out at a frequency of 1 Hz from 0 to 200 °C using an Anton Paar MCR 702e Multi Drive Rheometer (Graz, Austria) in tensile configuration testing rectangular 3D printed specimen with 50 mm of length, 10 mm of width, and 2 mm of thickness.

The tensile tests were also performed on seven 3D printed dog bone specimens according to the ISO 527-2-5A standard [32], using an Instron 5966 equipped with pneumatic grips and a 2 kN load cell, with a deformation rate of 5 mm min^{-1} and a grip separation of 50 mm.

Seven specimens were tested for each material type to provide statistically meaningful data.

2.5. Biocompatibility Evaluation

NIH3T3 fibroblast cells, derived from embryonic mouse (Mus musculus) fibroblasts, were obtained from the German Collection of Microorganisms and Cell Cultures (DSMZ, Braunschweig, Germany), and were seeded onto the surface of AESO-THFA-based polymers in a 20 μL droplet. This approach was used to prevent cells from sliding into the well area and to promote their adhesion to the polymer surface. The NIH3T3 mouse fibroblasts were cultured in a DMEM medium composed of Dulbecco's Modified Eagle's Medium high glucose with sodium pyruvate (Corning 15-017-CV), supplemented with 10% fetal bovine serum (SIAL yourSIAL-FBS-SA), L-glutamine 0.02 mM (Euroclone ECB3004D), and 10 U/mL penicillin/streptomycin (Euroclone ECB3001D). Confluent cells (80%) were sub-cultured routinely at a split ratio of 1:10 three times after trypsin/EDTA (Aurogene AU-X0930-100) digestion and cultured at 37 °C, 5% CO_2 in humified atmosphere to allow cell attachment. After this incubation period, each well of the multi-well plates was filled with 1 mL of complete DMEM medium, and the plates were returned to the incubator to support cell growth.

Before cell seeding, the AESO-based photocured specimens were prepared, placed for 15 min on a hot plate at a temperature of 150 °C and boiled in water at 100 °C for 1 h. After drying, they were sterilized by UV ray exposure for 1 h on each side.

NIH3T3 cells were seeded on the specimens at a cell density of 3500 cells/scaffold and were incubated at 37 °C, 5% CO_2, in humified atmosphere. At different time points (24, 48, 72 h), cell viability was determined by the resazurin reduction assay as previously reported [33].
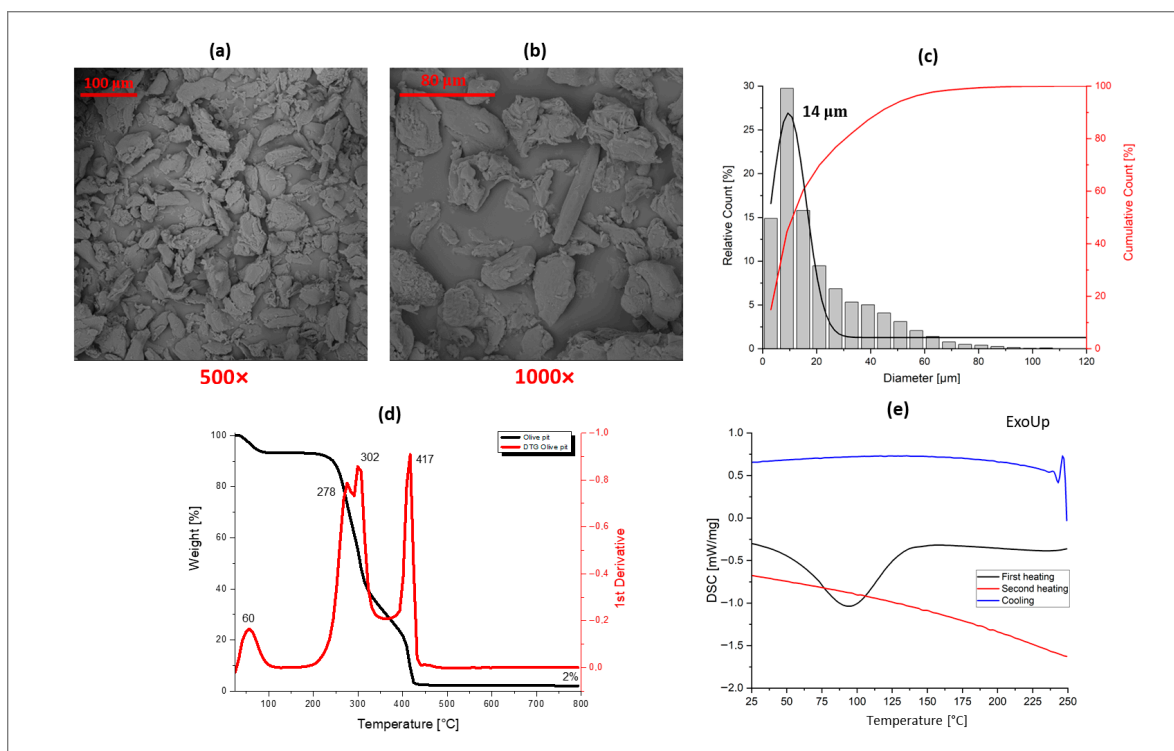
The samples were fixed for 20 min in 2.5% glutaraldehyde in DPBS (pH 7.4) and dehydrated through a graded series of alcohol (50%, 75%, 95%, 100%) for 15 min each. Then, the specimens were dried overnight and coated with gold-palladium (10 nm thickness) using an Emitech K550 sputter coater (Quorum Technologies, South Stour Avenue, Kent, UK). Samples were observed with the Nova NanoSEM 450 (Fei Company-Bruker corporation, Hillsboro, OR, USA). SEM images were taken under high-vacuum conditions using an Everhart Thornley Detector (ETD) with an accelerating voltage of 15 kV and a magnification of 600× and 1200×.

3. Results

3.1. Olive Pit Powder Characterization

OP powder morphology was evaluated by SEM analysis to study the shape and dimension of the particles. Figure 1a,b show SEM micrographs of the filler at 500× and 1000× magnification. The images reveal that OP powder appears compact and homogeneous, characterized by small particles with irregular shape and a dimension close to 20 microns. It is also evident that the OP particles tend to easily form agglomerates appearing as larger particles in the SEM image with a dimension lower than 100 microns. This can make it difficult to accurately determine the true size distribution of the particles, as the observed size reflects the agglomerated clusters rather than individual particles.

To assess particle size distribution, granulometric analysis was performed by analyzing thousands of olive pit particles having a representative view of the morphological features of the powder, as shown in Figure 1c. The average size of the powder is approximately 14 μm. The distribution profile indicates a predominantly uniform size range with minimal variance in particle dimension, confirming the presence of some aggregates that do not exceed 100 μm, as previously seen by SEM investigation.

Figure 1. SEM micrographs at 500× (**a**) and 1000× (**b**), particle size distribution (**c**), TG and DTG curves (**d**), and DSC curves (**e**) of olive pit.

This particle size distribution is of particular significance for AM applications because it suggests a homogenous potential dispersion of the filler within the photocurable polymeric matrix.

OP powder thermal behavior was studied by means of TG and DSC analyses. The TG and DTG curves of the olive pit powder are reported in Figure 1d and the DSC curves performed in nitrogen are displayed in Figure 1e. Looking at Figure 1d, the OP powder thermogram shows a typical thermal decomposition behavior of a lignocellulosic material which begins to be noticeable over 250 °C. It frequently presents two distinct peaks in the DTG curve which indicate that there should be at least two main reactions occurring during the degradation process, as the literature already reports [19,34].

Filler degradation implies a first degradation peak at around 60 °C due to the elimination of the water absorbed onto the powder surface, a broad degradation peak with a maxima of weight loss in the range between 278 and 302 °C attributed to the degradation of the fractions of hemicellulose and cellulose, and finally a main single degradation peak at 417 °C assigned to the lignin. The existence of these characteristic peaks has been already observed in many other filler thermal profiles [16,18,19]. The ash content of the OP was identified at 800 °C as 2%, relatively high compared with the residue of other pits, like cherry (0.25%) and nut shells (1%) but in line with the literature data [27,34–36].

Figure 1e also includes the DSC curves of the OP powder related to heating and cooling scans, from which only a peak at around 100 °C appears evident due to the moisture evaporation. No other exothermic or endothermic peaks are expected.

3.2. AESO-Based Photocurable Formulations

AESO-based mixtures containing 60 wt.% of AESO and 40 wt.% of THFA were prepared by LCD 3D printing. OP powder was dispersed within the liquid photocurable formulations at different concentrations, 5 and 7.5 wt.%, respectively. To study the effect of the filler's addition on resin flowability, the viscosity was evaluated considering that it

can significantly influence the processability for the VP 3D printing process. In fact, resin viscosity plays a crucial role during an LCD printing process because high viscosities result in longer printing times and lower rates [18,19,24]. To overcome the viscosity issue, the high AESO viscosity was significantly reduced by adding THFA to the photocurable resin. Table 1 shows the viscosity value comparison between the pristine AESO-THFA sample and the composites filled with different amounts of OP powder.

Table 1. Viscosity values of unfilled and filled AESO-based formulations with olive pit powder.

Sample Code	Viscosity @25 °C (mPa s)
AESO-THFA	377
AESO-THFA+O5	351
AESO-THFA+O7.5	353

The AESO-THFA system shows a viscosity value of 377 mPa·s. The viscosity decreases by increasing the olive pit powder content up to 7.5 wt.%. AESO-THFA+O5 and AESO-THFA+O7.5 manifest a value of viscosity of 351 mPa·s and 353 mPa·s at 1 1/s of shear rate, respectively. Olive pit powder is highly porous and can absorb high-viscosity components from the liquid AESO resin. This led the continuous phase to be richer in lower-viscosity diluents, reducing the overall viscosity. This effect is especially relevant if the resin contains reactive diluents like THFA [18]. However, the viscosity values are perfectly within the optimal range of viscosity for VP processing, according to the literature [18,19,33].
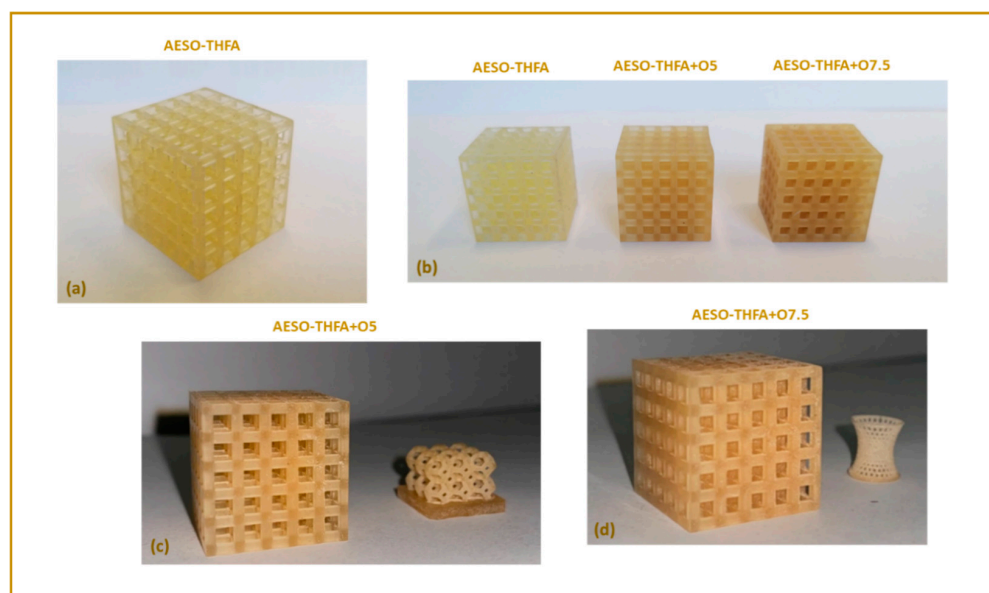
3.3. Three-Dimensional Printing Process via LCD

Different printing tests were first carried out to assess the effective printing parameters and the printability of the AESO-based resins via LCD. The best printing parameters for each formulation were found and are listed in Table 2.

Table 2. LCD printing parameters for AESO-based resins and composites.

Parameter	AESO-THFA	AESO-THFA+O5	AESO-THFA+O7.5
Layer height (mm)	0.1	0.1	0.1
Exposure time (s)	18	18	18
Bottom exposure time (s)	40	40	70
Rest time before lift (s)	0	0	1
Rest time after lift (s)	5	5	5
Rest time after retract (s)	3	3	3
Lifting distance (mm)	6	6	6
Retract distance (mm)	6	8	8
Lifting speed (mm/min)	90	90	90
Retract speed (mm/min)	170	170	170

Several AESO-based objects were 3D printed and then unfilled and filled with OP powder by LCD. Figure 2 shows typical structures realized by LCD, such as cube-shape lattices made of 400 layers, honeycomb-like shapes (100 layers), and knitted wire mesh structures (100 layers). All the AESO-based samples evidence high resolution and accuracy, good layer adhesion, and detailed definition. The 3D printed objects containing OP powder display a significant change in color induced by the presence of the filler, which acts as a dye agent, as evidenced by Figure 2b,c.

Figure 2. Three-dimensional printed AESO-based objects unfilled (**a**) and filled with different amounts of olive pit powder (**b**–**d**).

3.4. Insoluble Fraction

The insoluble fraction of the photocured AESO-based samples, evaluated after 24 h extraction in chloroform, shows values higher than 99% (see Table 3), underlining that the addition of OP powder within the AESO-THFA matrix does not influence the crosslinked polymer network.

Table 3. Gel content and thermal properties of the unfilled and filled AESO-based formulations with olive pit powder.

Sample Code	Gel (%)	T_{onset} (°C)	$T_{max\ deg\ peak}$ (°C)	Residue (wt.%)	T_g (°C)
AESO-THFA	99.2	317	406/562	0	5
AESO-THFA+O5	99.4	307	403/572	1	11
AESO-THFA+O7.5	99.6	298	403/561	2	13

This highlights that the printing parameters are optimized for obtaining an almost compete conversion of the monomers into the LCD 3D printer.

3.5. Morphology of AESO-Based 3D Printed Samples

A morphological investigation was carried out to study the microstructure of the AESO-based 3D printed samples by SEM. The micrographs, at 1000× magnification reported in Figure 3, show an even distribution of the OP powder within the AESO-THFA photocured resin. This suggests that the filler is well distributed within the resin, resulting in good printing quality. Additionally, it indicates that no particle sedimentation occurred during the printing process.
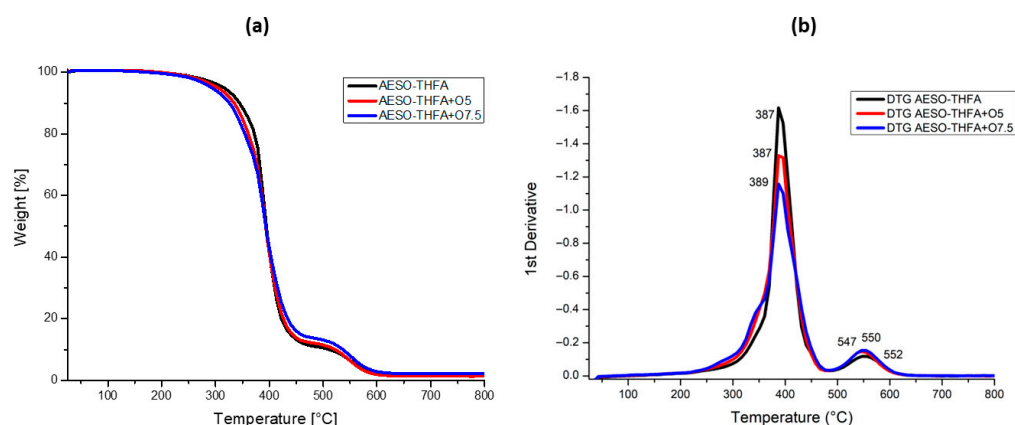
However, some little voids close to the borders of the specimens are present, as evidenced by the three yellow arrows reported in Figure 3b. They underline the tendence of the filler's particles to form agglomerates within the AESO resin and the low interaction between the filler and the polymer matrix that, however, do not significantly compromise the printing process.

Figure 3. SEM images of 3D printed AESO-THFA unfilled (**a**) and filled with olive pit powder, O5 (**b**) and O7.5 (**c**).

3.6. Thermal and Viscoelastic Properties of AESO-Based 3D Printed Samples

The thermal stability of the AESO-based 3D printed samples was evaluated by means of TGA analysis. Figure 4 reports the TG curves of the samples obtained by adding THFA as diluent and the unfilled and filled with different concentrations of OP powder, 5 and 7.5 wt.%, respectively.

Figure 4. TG (**a**) and DTG (**b**) curves of 3D printed samples unfilled or filled with olive pit powder.
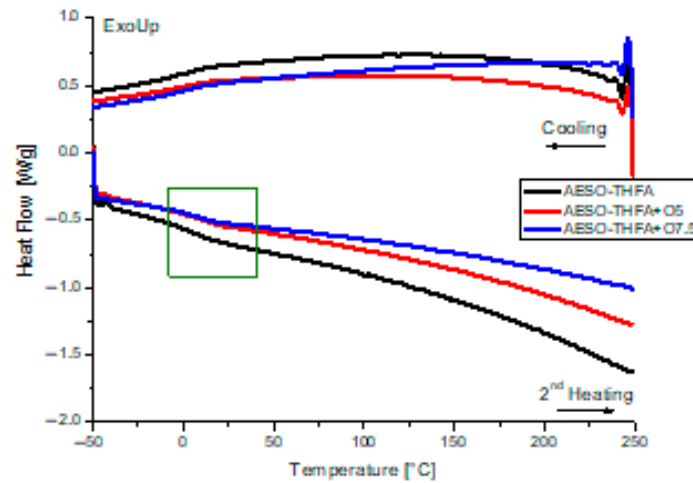
The thermograms of Figure 4a show almost the same thermal behavior to highlight that the addition of OP powder to the AESO-THFA does not have an effect on thermal stability, which remains almost the same. The thermal degradation for all the printed samples involves two main steps, as visible from DTG curves reported in Figure 4b.

The first degradation step occurs at around 387 °C while the second degradation stage occurs at a temperature close to 550 °C for all the 3D printed samples. The onset temperature instead slightly shifts toward lower values by increasing the amount of olive pit powder, from 317 °C for the neat AESO-THFA sample to 298 °C for the composites filled with 7.5 wt.% of filler (see Table 3).

This can be explained considering that the particle presence slightly influences the initial stage of degradation, in agreement with the observations of other authors [2,29]. Moreover, a small ash content was found at 800 °C for the samples filled with OP powder due to presence of inorganic compounds within the filler chemical composition, as visible from Table 3.
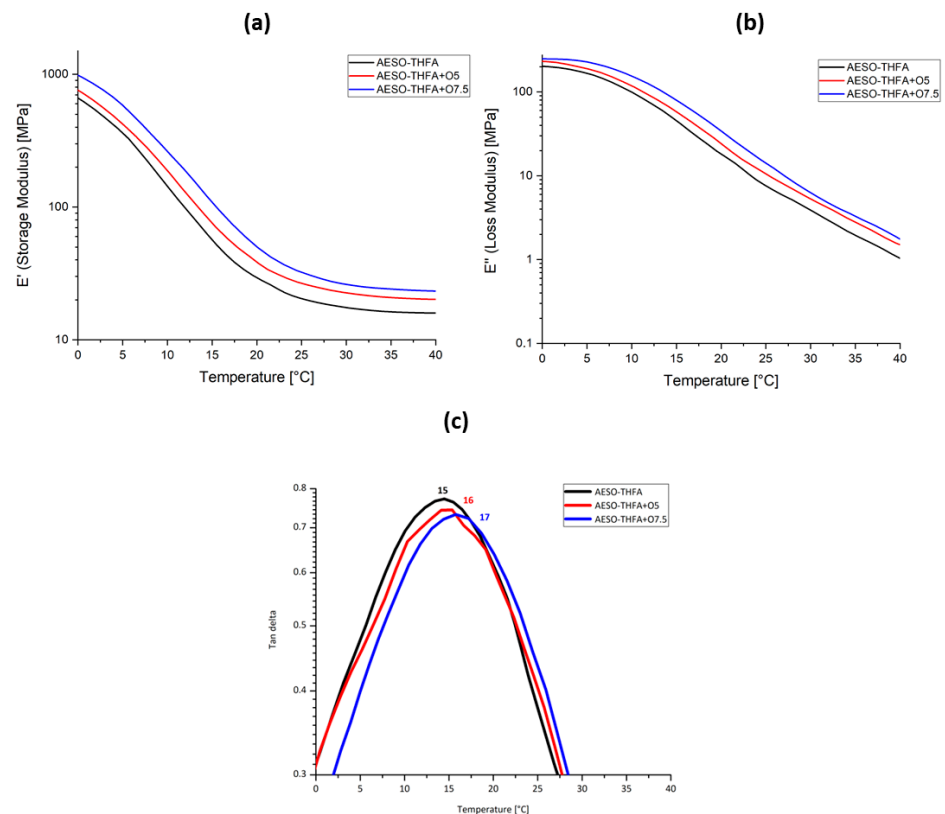
The DSC curves, performed in nitrogen and reported in Figure 5, show that the glass transition temperature of the AESO-based 3D printed samples, evaluated on the second heating scan, slightly increases by adding OP powder to the polymeric system, from 5 °C for the unfilled AESO-THFA to 11 and 13 °C for the composite containing 5 and 7.5 wt.% of

filler, respectively (see Table 3). This result can be assigned to the reinforcing effect induced by the addition of the OP powder within the AESO-based matrix. In fact, the presence of filler particles can slightly hinder the segmental motion of the polymeric chains inducing a little increase in glass transition temperature values by increasing filler content.

Figure 5. DSC curves of 3D printed samples unfilled or filled with olive pit powder. The box evidences the glass transition temperature.

Moreover, the effect of the addition of OP powder within the AESO-based resin was also investigated from thermo-mechanical and mechanical point of views. DMA allows evaluation of the storage (E') and loss (E'') moduli, as well as tan delta values for the neat AESO-THFA samples and the bio-based composites, as shown in Figure 6.

Figure 6. DMA curves of 3D printed samples unfilled or filled with olive pit powder showing the storage modulus (**a**), loss modulus (**b**), and tan delta (**c**).

The storage modulus values, recorded in the glassy region at 0 °C, shift from 624 MPa for the pristine AESO-THFA sample to 728 and 947 MPa for the samples containing 5 and 7.5 wt. % of OP powder to underline a stiffening effect induced to the presence of the filler, as visible from Figure 6a. The same trend was observed at room temperature in the rubbery plateau, where the storage modulus values shifted from 8 MPa for the unfilled system up to 15 MPa for the sample loaded with 7.5 wt.% of agro-waste powder. By comparing the loss moduli for the pristine sample and those of the composites, it is possible to see a similar behavior both in the rubbery region (at 25 °C) and in the glassy one (at 0 °C) consisting in an increase in the values when increasing the olive pit powder content up to 7.5 wt.%, as visible in Figure 6b. The E″ increases from 210 MPa to 245 MPa at 0 °C and from 21 to 33 MPa at 25 °C, as summarized in the data of Table 4. Thus, the addition of filler makes the polymer more rigid and brittle as confirmed by the E′ and E″ moduli increments.

Table 4. Viscoelastic and tensile properties of samples unfilled and filled with olive pit powder.

Sample Code	E′ [a] (MPa)	E″ [a] (MPa)	E′ [b] (MPa)	E″ [b] (MPa)	Tan δ (°C)	Young's Modulus (MPa)	Ultimate Tensile Strength (MPa)	Elongation at Break (%)
AESO-THFA	670	210	8	21	15	12.7 ± 1.0	0.8 ± 0.2	7.0 ± 0.8
AESO-THFA+O5	728	238	11	27	16	13.5 ± 0.5	0.7 ± 0.1	6.6 ± 0.6
AESO-THFA+O7.5	947	245	15	33	17	13.9 ± 0.4	0.7 ± 0.1	5.8 ± 0.9

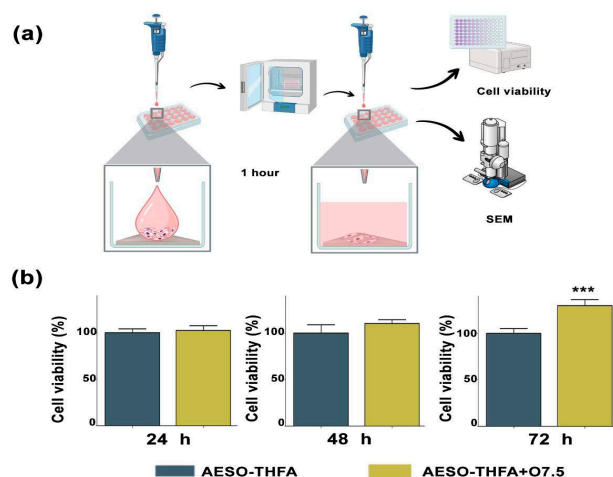[a] E′ and E″ values determined by DMA curves at 0 °C. [b] E′ and E″ values determined by DMA curves at 25 °C.

This can be explained by considering the reinforcing effect due to the OP particles, thus slightly enhancing the mechanical response of the system [37]. From DMA, it was also possible to determine the glass transition temperature (T_g) values evaluating the maximum of tan delta curves as a function of the temperature reported in Figure 6c. The T_g values do not vary in the presence of OP powder. The tan delta curves show almost the same trend with a very broad profile.

Finally, tests were performed to investigate the tensile properties of the printed specimens. The addition of OP powder led to a small increase in the elastic modulus values due once again to the filler particle presence, confirming the previous DMA results. Moreover, the filler seems to slightly decrease the tensile strength and elongation at break, revealing little enhancement of the stiffness of the polymer and a decrease in the ductility [37].

3.7. Biocompatibility of AESO-Based 3D Printed Samples

The biocompatibility of the 3D printed samples was assessed by using NIH3T3 mouse fibroblast cells, preventing cells from sliding into the well area and promoting their adhesion to the polymer surface, employing the approach sketched in Figure 7a. The cells adhered to both materials as early as 1 h after seeding. Cell viability was then assessed at 24, 48, and 72 h. At 24 and 48 h, no significant differences in cell adhesion and viability were observed between AESO-THFA and AESO-THFA+O7.5. However, after 48 h, a slight increase in cell viability on AESO-THFA+O7.5 was already noticeable compared to the neat AESO-THFA polymer. Then, after 72 h of culture, a significant increase in cell proliferation was observed in AESO-THFA+O7.5 compared to AESO-THFA, as visible in Figure 7b, indicating that the AESO-THFA+O7.5 sample prepared by adding the filler was more capable of stimulating fibroblast cell adhesion and growth.
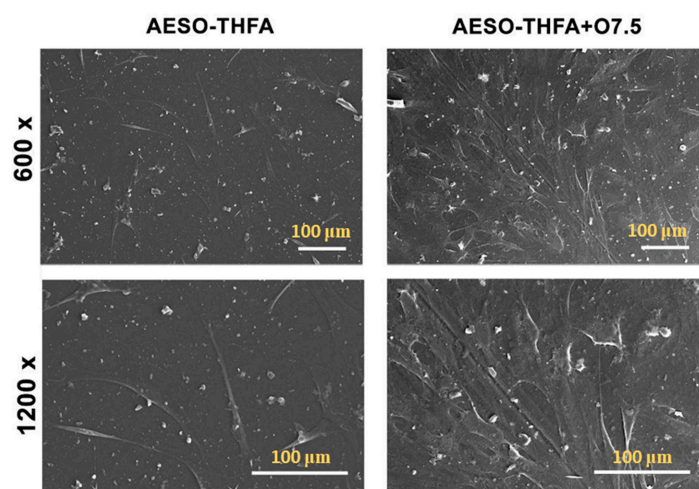
Figure 7. Cell seeding procedure scheme. Seeding was performed by placing a drop with DMEM full medium containing the cells on the polymer surfaces (**a**). After 1 h of incubation, the cells adhered to the polymer and each well was filled with DMEM full medium for further investigation, cell viability, and SEM analyses (**b**). *** is *p*-value < 0.001.

The addition of olive pit powder to the AESO-based formulations can help enhance the adhesion and growth of the fibroblast cells probably due to the combination of several interconnected physicochemical and biological factors.

Olive pit powder, present within the AESO-THFA+O7.5 specimen, introduces micro-roughness onto the polymer surface by increasing the surface area and roughness and providing more anchoring points for cell attachment, which promotes a better cell adhesion.

Moreover, olive pit powder, being a natural, non-toxic, and biodegradable material, contains several natural bioactive compounds, such as polyphenols and lignocellulosic materials that can improve the protein adsorption, a key step in cell adhesion and proliferation. As visible from the histograms of Figure 7b, the cell viability reaches 100% in the presence of the highest amount of filler, accompanied by a remarkable increase after 72 h of culture. These effects were particularly evident in SEM images taken at 72 h from seeding (Figure 8). In fact, morphological analysis revealed that cells grown on AESO-THFA+O7.5 adhered in greater numbers, exhibiting a well-spread and flattened morphology on the material surface. In contrast, cells on AESO-THFA appeared more elongated, less flattened, and with lower proliferative activity.

Figure 8. Morphological observations by SEM analysis were performed and images were taken after 72 h at 600× and 1200× magnification (scale bar = 100 μm).

4. Conclusions

The present work highlights the possibility to prepare bio-based polymeric composites by dispersing different amounts of OP powder up to 7.5 wt.% within an AESO-based resin and using LCD as vat photopolymerization technology.

This research aims to propose an alternative way to bring the full potential of agro-waste-based composites for possible applications into the biomedical field using 3D printing as a greener manufacturing method. Once printing parameters are optimized, different geometries are realized by adding OP to the AESO-THFA formulation in a very short time. Cube-shape lattices, honeycomb-like shapes, and wire mesh structures are successfully developed showing singular structures and very high dimensional definition. The composites are then fully characterized from morphological, thermal, and mechanical points of view.

The results obtained reveal that the addition of OP powder as filler within the AESO-based matrix induces a slight increase in the T_g values and the elastic modulus, underlining the stiffening effect induced in filler presence. The thermal stability remains almost the same after the printing process, suggesting that olive pit powder does not influence the thermal behavior of the AESO-THFA system. The reinforcing effect due to the olive pit particles also reveals that the filler particles are well distributed inside the matrix, thus enhancing the mechanical response of the polymeric system, although showing some little agglomerate. Considering these findings, biocompatibility and cell growth on polymer and polymeric composites are further evaluated, finding that the material promotes cell adhesion and that viability is improved in the presence of olive pit extract (AESO-THFA+O7.5) compared to AESO-THFA alone, suggesting a potential novel role for this filler in biomedical applications.

This study certainly deserves further investigation, but the proposed approach to develop novel bio-based composites filled with OP has the potential to substantially expand the use of renewable materials into the 3D printing field for realizing components for biomedical applications, employing LCD as a vat polymerization technology. Moreover, the combination of 3D printing and the valorization of fillers coming from agricultural waste can offer a great opportunity to reduce the raw material costs and encourage the design and development of a novel generation of more eco-friendly 3D printed composite materials.

References

1. Russo, G.; Beritognolo, I.; Bufacchi, M.; Stanzione, V.; Pisanelli, A.; Ciolfi, M.; Lauteri, M.; Brush, S.B. Advances in biocultural geography of olive tree (*Olea europaea* L.) landscapes by merging biological and historical assays. *Sci. Rep.* **2020**, *10*, 7673. [CrossRef]
2. Valvez, S.; Maceiras, A.; Santos, P.; Reis, P.N.B. Olive Stones as Filler for Polymer-Based Composites: A Review. *Materials* **2021**, *14*, 845. [CrossRef]
3. García Martín, J.F.; Cuevas, M.; Feng, C.H.; Mateos, P.Á.; García, M.T.; Sánchez, S. Energetic valorisation of olive biomass: Olive-tree pruning, olive stones and pomaces. *Processes* **2020**, *8*, 511. [CrossRef]
4. Nunes, M.A.; Pimentel, F.B.; Costa, A.S.G.; Alves, R.C.; Oliveira, M.B.P.P. Olive by-products for functional and food applications: Challenging opportunities to face environmental constraints. *Innov. Food Sci. Emerg. Technol.* **2016**, *35*, 139–148. [CrossRef]
5. Rodríguez, G.; Lama, A.; Rodríguez, R.; Jiménez, A.; Guillén, R.; Fernández-Bolaños, J. Olive stone an attractive source of bioactive and valuable compounds. *Bioresour. Technol.* **2008**, *99*, 5261–5269. [CrossRef]
6. Sánchez-Borrego, F.J.; de Hoyos-Limón, T.J.B.; García-Martín, J.F.; Álvarez-Mateos, P. Production of Bio-Oils and Biochars from Olive Stones: Application of Biochars to the Esterification of Oleic Acid. *Plants* **2022**, *11*, 70. [CrossRef]
7. Ortega, F.; Versino, F.; López, O.V.; García, M.A. Biobased composites from agro-industrial wastes and by-products. *Emergent Mater.* **2022**, *5*, 873–921. [CrossRef]
8. D'Eusanio, V.; Marchetti, A.; Pastorelli, S.; Silvestri, M.; Bertacchini, L.; Tassi, L. Exploring Olive Pit Powder as a Filler for Enhanced Thermal Insulation in Epoxy Mortars to Increase Sustainability in Building Construction. *AppliedChem* **2024**, *4*, 192–211. [CrossRef]
9. Calovi, M.; Rossi, S. Functional Olive Pit Powders: The Role of the Bio-Based Filler in Reducing the Water Uptake Phenomena of the Waterborne Paint. *Coatings* **2023**, *13*, 442. [CrossRef]
10. Vandamme, E.J. Agro-industrial residue utilization for industrial biotechnology products. In *Biotechnology for Agro-Industrial Residues Utilisation*; Springer: Berlin/Heidelberg, Germany, 2009; pp. 3–11.
11. Gullon, P.; Gullon, B.; Astray, G.; Carpena, M.; Fraga-Corral, M.; Prieto, M.A.; Simal-Gandara, J. Valorization of by-products from olive oil industry and added-value applications for innovative functional foods. *Food Res. Int.* **2020**, *137*, 109683. [CrossRef]
12. Jurado-Contreras, S.; Navas-Martos, F.J.; Rodríguez-Liébana, J.A.; Moya, A.J.; La Rubia, M.D. Manufacture and Characterization of Recycled Polypropylene and Olive Pits Biocomposites. *Polymers* **2022**, *14*, 4206. [CrossRef]
13. Saleem, J.; Shahid, U.B.; Hijab, M.; Mackey, H.; McKay, G. Production and applications of activated carbons as adsorbents from olive stones. *Biomass Convers. Biorefin.* **2019**, *9*, 775–802. [CrossRef]
14. Bhatnagar, A.; Kaczala, F.; Hogland, W.; Marques, M.; Paraskeva, C.; Papadakis, V.; Sillanpää, M. Valorization of solid waste products from olive oil industry as potential adsorbents for water pollution control—A review. *Environ. Sci. Pollut. Res.* **2014**, *21*, 268–298. [CrossRef]
15. Saroia, J.; Wang, Y.; Wei, Q.; Lei, M.; Li, X.; Guo, Y.; Zhang, K. A review on 3D printed matrix polymer composites: Its potential and future challenges. *Int. J. Adv. Manuf. Technol.* **2020**, *106*, 1695–1721. [CrossRef]
16. Koutsomitopoulou, A.F.; Bénézet, J.C.; Bergeret, A.; Papanicolaou, G.C. Preparation and characterization of olive pit powder as a filler to PLA-matrix bio-composites. *Powder Technol.* **2014**, *255*, 10–16. [CrossRef]
17. Yoha, K.S.; Moses, J.A. 3D Printing Approach to Valorization of Agri-Food Processing Waste Streams. *Foods* **2023**, *12*, 212. [CrossRef]
18. Colucci, G.; Sacchi, F.; Bondioli, F.; Messori, M. Fully Bio-Based Polymer Composites: Preparation, Characterization, and LCD 3D Printing. *Polymers* **2024**, *16*, 1272. [CrossRef]
19. Colucci, G.; Sacchi, F.; Bondioli, F.; Messori, M. 3D printing of lignin-based polymeric composites obtained using liquid crystal display as a vat photopolymerization technique. *Polym. Int.* **2025**, *74*, 828–838. [CrossRef]
20. Ligon, S.C.; Liska, R.; Stampfl, J.; Gurr, M.; Mu, R. Polymers for 3D Printing and Customized Additive Manufacturing. *Chem. Rev.* **2017**, *117*, 10212–10290. [CrossRef]
21. Sanchez-Rexach, E.; Johnston, T.G.; Jehanno, C.; Sardon, H.; Nelson, A. Sustainable Materials and Chemical Processes for Additive Manufacturing. *Chem. Mater.* **2020**, *32*, 7105–7119. [CrossRef]
22. Thakar, C.M.; Parkhe, S.S.; Jain, A.; Phasinam, K.; Murugesan, G.; Joy, R.; Ventayen, M. 3d Printing: Basic principles and applications. *Mater. Today Proc.* **2022**, *51*, 842–849. [CrossRef]
23. Alammar, A.; Kois, J.C.; Revilla-León, M.; Att, W. Additive Manufacturing Technologies: Current Status and Future Perspectives. *J. Prosthodont.* **2022**, *31*, 4–12. [CrossRef] [PubMed]
24. Sacchi, F.; Colucci, G.; Bondioli, F.; Sangermano, M.; Messori, M. Review: Bio-based photopolymers for additive manufacturing. *J. Mater. Sci.* **2025**, *60*, 11191–11220. [CrossRef]
25. Voet, V.S.D.; Guit, J.; Loos, K. Sustainable photopolymers in 3D printing: A review on biobased, biodegradable, and recyclable alternatives. *Macromol. Rapid Commun.* **2021**, *42*, e2000475. [CrossRef]

26. Skliutas, E.; Lebedevaite, M.; Kasetaite, S.; Rekštytė, S.; Lileikis, S.; Ostrauskaite, J.; Malinauskas, M. A Bio-Based Resin for a Multi-Scale Optical 3D Printing. *Sci. Rep.* **2020**, *10*, 9758. [CrossRef]

27. Lastovickova, D.N.; Toulan, F.R.; Mitchell, J.R.; VanOosten, D.; Clay, A.M.; Stanzione, J.F.; Palmese, G.R.; La Scala, J.J. Resin, cure, and polymer properties of photopolymerizable resins containing bio-derived isosorbide. *J. Appl. Polym. Sci.* **2021**, *138*, 50574. [CrossRef]

28. Chebotar, A.; Domnich, B.; Panchenko, Y.; Donchak, V.; Stetsyshyn, Y.; Voronov, A. Thermal behavior of polymers and copolymers based on plant oils with differing saturated and monounsaturated content. *Polym. Int.* **2024**, *74*, 255–263. [CrossRef]

29. Porcarello, M.; Mendes-Felipe, C.; Lanceros-Mendez, S.; Sangermano, M. Design of acrylated epoxidized soybean oil biobased photo-curable formulations for 3D printing. *Sustain. Mater. Technol.* **2024**, *40*, e00927. [CrossRef]

30. Lebedevaite, M.; Gineika, A.; Talacka, V.; Baltakys, K.; Ostrauskaite, J. Development and optical 3D printing of acrylated epoxidized soybean oil-based composites with functionalized calcium silicate hydrate filler derived from aluminium fluoride production waste. *Compos. Part A* **2022**, *157*, 106929. [CrossRef]

31. *ASTM D2765-84*; Standard Test Methods for Determination of Gel Content and Swell Ratio of Crosslinked Ethylene Plastics. ASTM International: West Conshohocken, PA, USA, 1984.

32. *ISO 527-2:2025*; Plastics—Determination of Tensile Properties—Part 2: Test Conditions for Moulding and Extrusion Plastics. International Organization for Standardization (ISO): Geneva, Switzerland, 2025.

33. Barbalinardo, M.; Biagetti, M.; Valle, F.; Cavallini, M.; Falini, G.; Montroni, D. Green Biocompatible Method for the Synthesis of Collagen/Chitin Composites to Study Their Composition and Assembly Influence on Fibroblasts Growth. *Biomacromolecules* **2021**, *22*, 3357–3365. [CrossRef]

34. Marcilla, A.; García, A.N.; Pastor, M.V.; León, M.; Sánchez, A.J.; Gómez, D.M. Thermal decomposition of the different particles size fractions of almond shells and olive stones. Thermal behaviour changes due to the milling processes. *Thermochim. Acta* **2013**, *564*, 24–33. [CrossRef]

35. Shogren, R.L.; Petrovic, Z.; Liu, Z.; Erhan, S.Z. Biodegradation behavior of some vegetable oil-based polymers. *J. Polym. Environ.* **2004**, *12*, 173–178. [CrossRef]

36. Barkane, A.; Platnieks, O.; Jurinovs, M.; Gaidukovs, S. Thermal stability of UV cured vegetable oil epoxidized acrylate-based polymer system for 3D printing application. *Polym. Degrad. Stabil.* **2020**, *181*, 109347. [CrossRef]

37. Reis, P.N.B.; Ferreira, J.A.M.; Silva, P.A.A. Mechanical Behaviour of Composites Filled by Agro-waste Materials. *Fibers Polym.* **2011**, *12*, 240–246. [CrossRef]